https://doi.org/10.26682/ajuod.2022.25.1.4
Journal of University of Duhok., Vol. 25, No.1 (Agri. and Vet. Sciences), Pp 26-37, 2022

APPLICATION OF GEOSPATIAL TECHNIQUES IN ANALYST DISTRIBUTION PATTTERN OF SOME SOIL PROPERTIES IN ERBIL PROVINCE, KURDISTAN REGION-IRAQ

HAWAR ABDULRZAQ SADIQ RAZVANCHY* and MOHAMMED ALI FAYYADH**
*Soil and Water Sciences, College of Agricultural Engineering Sciences, University of Salahaddin, Kurdistan Region-Iraq
**Soil and Water Sciences, College of Agricultural Engineering Sciences, University of Duhok, Kurdistan Region-Iraq

(Received: October 21, 2021; Accepted for Publication: January 6, 2022)

ABSTRACT

The study area is located in Erbil province, Kurdistan region, Iraq (that extends from Latitude 35.436151N to 37.319894N and from Longitude 43.374316E to 45.080122E) and aimed explain the distribution of some soil properties depending on geospatial techniques. Fourteen geo-referenced soil pedons have been elected. The ArcMap 10.7 software has been used in this study. Bulk density generally increases with depth in studied pedons. Interpolated map for distribution of clay particles, appears the higher values of clay particles and fine soil texture are located at the north, northwest, and decreasing into the south, southwest. Clay content has different distribution patterns. An alkaline studied soil pH with low salts content. Organic matter and total carbonate decreased with depth and an increase pedogenic carbonate that has a positive significant correlation with both slope and elevation. Active carbonate has a strong correlation with clay particles. Soil gypsum and total nitrogen decreased with depth in most pedons. The study concluded that decreasing into the south and southwest. Soil organic matter tends to increase as the clay content increases and higher values of organic matter content are located at northwest and decreasing gradually to south and southwest. Soils have different distribution patterns of total and active carbonates along pedons. CEC decreased from northwest toward a southeast.

***KEYWORDS*:** Horizons, Pedon, Rainfall, Spatial Variability, Topography,

1. INTRODUCTION

Soil properties are the most important factors that have great effects on the quantity and quality of vegetation covers (Al-Quraishi et al., 2020). The information on spatial soil variability is critical in agriculture to aid farmers in making agronomic farm management decisions. This aims to assure high agricultural yields and cheap production costs while minimizing unexpected environmental consequences (Baharom et al., 2015). One of the most important factors influencing soil formation and development is the climate (Ismail, 2013). Soil properties development may be recorded as a result of climate changes (Bockheim et al., 2000). Topographic diversity can also cause variations in soil characteristics within a particular climatic area (Brubaker et al., 1993). As a result, the relationship between topography and soil characteristics has been widely researched (Kravchenko and Bullock, 2000). Correspondingly, Kumhálová et al., (2011) considered that elevation and slope are important topographical factors those affecting soil properties. According to Iqbal et al., (2005) topographic changes influence the locational variance of soil characteristics and agricultural yields. The study of soil properties variability with depth or vertical variability has been ignored through many researchers that studied the distribution of soil properties (Baharom et al., 2015), conversely to this, Donovan (2012) reported that soil properties changes dramatically with depth even starts with the few centimeters under the topsoil. The aims of this study is to identify how the soil properties change horizontally and vertically in Erbil province with finding the major causes for these changes. As well as, to explore the interrelationship between soils physicochemical properties with topographical and climatic (rainfall and temperature) criteria and to what extent are they influencing each other.

hawar.sadiq@su.edu.krd

Furthermore, a map of the studied soil properties is prepared to illustrate their spatial variability.

2. MATERIALS AND METHODS

2.1 Study area and sampling

The study area is located at Erbil province, Kurdistan region, Iraq with an area of 14,485 km^2, and the geographical position extends from Latitude 35.436151N to 37.319894N and from Longitude 43.374316E to 45.080122E (Figure 1). Fourteen geo-referenced soil pedons have been selected depending on the latitude and longitude with specifying elevation and slope (Table 1). Forty-one soil samples were collected from horizons in study pedons then air-dried, crushed, and sieved with a 2 mm sieve after that were kept in plastic containers for physical and chemical analyses.

2.2 Topographical criteria

A mosaic of two Shuttle Radar Topography Mission (SRTM) 1 arc-second Digital Elevation Model (DEM) have been used, these images are downloaded from https://glovis.usgs.gov/app. The DEM raster dataset of the study area was used to confirm the slopes and elevations values that have been taken during field works for each soil samples location with digital numbers values (DN values). For this purpose, the Extraction function has been utilized using ArcGIS software version 10.7. The Mean of slopes and elevations have been calculated and used as topographic parameters from those data that have been taken during field observation and from the DEM.

2.3 Meteorological criteria

Both rainfall and temperature data have been collected from 22 rain gauges stations and 12 meteorological stations across the study area which is provided by the Erbil province meteorological directory. Both rainfall and temperature values have been generalized to cover the study area, for this purpose, the interpolated maps have been generated for both then the values of temperature and rainfall have been extracted for soil pedons location. The average yearly rainfall amount for (14) years (2006-2020) was (1390.1, 635.5, 776.4, 740.8, 376.6, 538.6, and 240.6) mm in districts of Mergasor, Soran, Choman, Shaqlawa, Erbil city, Koya, and Makhmour respectively. The average yearly temperature for (10) years (2010-2019) was (15.7, 18.3, 15.3, 17.7, 21.1, 22.1, and 24.1) C^o in the previous locations respectively.

2.4 Laboratory Analyses

Soil particles size distribution is determined using hydrometer method according Gee and Bauder, (1986). The bulk density was determined using wax method according to Black, (1980). The pH and electrical conductivity (EC) of the soil suspension (1:3) (soil: water) was measured by a pH meter and EC meter (Rowell, 1994). Soil organic matter was determined by wet combustion (Black, 1980). Total and active carbonate was determined by the titration method as described by Rowell, (1994) and Kozhekov and Yakovleva, (1977) respectively. Cation exchange capacity was measured by using Sodium acetate as described in Carter and Gregorich, (2007). Exchangeable calcium, magnesium, sodium, and potassium were measured as described in Rowell, (1994). Gypsum content was determined by the gypsum simulation (OMRAN GypSim) model (Congalton and Green, 2019). Total nitrogen was determined by the Kjeldahl apparatus (Bremner and Malvaney, 1982).

2.5 Interpolated maps

The interpolated maps were produced for all the soil properties as measured interpolated maps using the soil pedons upper horizon for this purpose the ArcMap software version 10.7. has been utilized. Geostatistical Analyst has been used based on the Kriging/CoKriging method ("Ordinary" type) as a method for producing the interpolated maps, as well as, the output maps divided into different classes depending on the magnitude of variation using the Geometrical Interval method for most of them.

The accuracy of all interpolated maps in this study has been determined using Root Mean Square Error (RMSE). In this study the RMSE, consider as degree of errors for each map, in another meaning, it shows the error values of the areas among soil samples. For instance, the value of RMSE is (0.217) in the bulk density map (Figure 2), it means that the maximum error of the predicted values for the areas among soil samples in this map probable smaller or greater by (0.217) according to their original or laboratorial values (Hyndman and Koehler, 2006). And so on for the other maps. The RMS's have been extracted from Cross-Validation/Prediction Errors in the final step of the interpolation process using the ArcMap software version 10.7. Each RMS's have been written beside the name of each interpolated map.

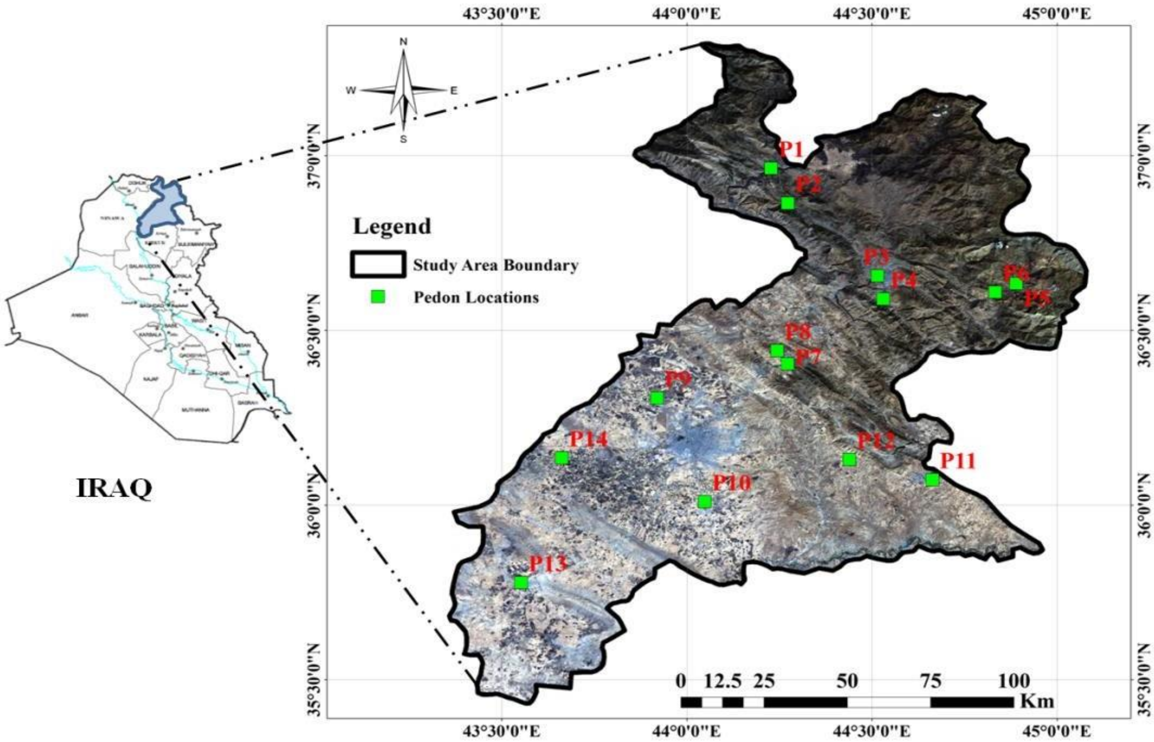

Fig. (1): The *study* area's map and the spatial distribution of soil pedons

Table (1): Elevation and slope of soil pedon sites.

Pedon number	Locations Name	Latitude	Longitude	Elevation (m)	Slope (%)
1	Chame	36° 57' 49.55"	44° 13' 40.23"	570	18.13
2	Goratu	36° 51' 49.65"	44° 16' 24.33"	950	5.40
3	Soran	36° 39' 21.25"	44° 30' 54.39"	605	8.59
4	Ruanduz	36° 35' 23.71"	44° 31' 49.64"	711	24.99
5	Choman	36° 38' 02.25"	44° 53' 23.16"	1109	31.20
6	Galala	36° 36' 34.13"	44° 49' 59.09"	968	19.72
7	Sheraswar	36° 24' 15.08"	44° 16' 21.41"	853	2.56
8	Shaqlawa	36° 26' 30.64"	44° 14' 40.22"	782	10.25
9	Gazna	36° 18' 22.99"	43° 55' 12.90"	365	1.81
10	Qushtapa	36° 00' 32.66"	44° 02' 55.64"	405	4.89
11	Koya	36° 04' 21.09"	44° 39' 49.99"	570	2.43
12	Bawa qub	36° 07' 49.49"	44° 26' 22.69"	711	3.08
13	Makhmour	35° 46' 39.79"	43° 33' 10.69"	254	4.62
14	Kawr	36° 08' 05.04"	43° 39' 45.38"	263	1.62

hawar.sadiq@su.edu.krd

2.6 Statistical analysis

The correlation coefficients (r) were calculated among soil physicochemical properties (surface samples results), DEM-derived data (slope and elevation), rainfall data, and temperature data. For this purpose, the Bivariate Correlations (Pearson Correlation Coefficient) as a default method was adopted. To find if the variables are related to one another. It is common to measure how those two variables simultaneously change together (Babbie, 2009).

3. RESULTS AND DISCUSSION

3.1 Physical properties

3.1.1 Bulk density

The laboratory results of soil physical properties, except for pedons (2 and 10) appear the bulk density generally increases with depth in all horizons (Table 2). These increases because of the compaction process by the upper horizons weight on the lower horizon in turn decrease the porosity and increase bulk density. Additionally, due to decrease of the organic matter with depth. Bulk density has a positive correlation with clay content, as well as, it has a negative significant correlation with the porosity. The maximum value of bulk density is (2.03 Mg/m^3) in C_k1 horizon of pedon (12). Moreover, the minimum is (1.42 Mg/m^3) in horizon A_p of pedon (13). Figure (2) shows the interpolated map for the distribution of soil bulk density, the higher bulk density is located in the north of the study area and

Table (2): Laboratory results for soil physical properties

Pedon no.	Horizon	Depth (cm)	**PSD ($g.kg^{-1}$)			*Texture Class	B. Density ($Mg.kg^{-1}$)
			Sand	Silt	Clay		
1	A_a	0 - 30	354	190	456	C	1.72
	C_k1	30 - 80	401	283	316	CL	1.74
	C_k2	80 - 120	401	338	261	L	2.01
2	A	0 - 40	400	241	359	CL	1.83
	C_k1	40 - 92	451	344	205	L	1.73
	C_k2	92 - 140	506	365	129	L	1.53
3	A_p	0 - 46	366	254	380	CL	1.54
	B_k	46 - 126	372	229	399	CL	1.86
4	A_p	0 - 25	263	258	479	C	1.67
	B_{tk}	25 - 57	254	225	521	C	1.79
	C_k	57 - 147	373	216	411	C	1.86
5	A_a	0 - 25	673	202	125	SL	1.63
	$C_{hk}1$	25 - 50	595	200	205	SCL	1.70
	C_k2	50 - 120	615	214	171	SL	1.43
6	A	0 - 28	564	220	216	SCL	1.44
	C_k1	28 - 66	600	175	225	SCL	1.50
	C_k2	66 - 101	641	191	168	SL	1.62
7	A_a	0 - 65	451	255	294	SCL	1.78
	B_{tk}	60 - 102	256	278	466	C	1.92
8	A	0 - 32	466	379	155	L	1.65
	B_{tk}	32 - 109	479	290	231	L	1.76
	C_k	109 - 179	559	298	144	SL	1.72
9	A_p	0 - 35	251	393	356	CL	1.60
	B_{hk}	35 - 100	272	348	380	CL	1.72
	C_k	100 - 147	256	355	389	CL	1.71
10	A_p	0 - 23	366	420	214	L	1.86
	$B_{tk}1$	23 - 81	266	391	343	CL	1.86
	$B_{tk}2$	81 - 135	276	383	341	CL	1.71
11	A_p	0 - 20	309	432	259	L	1.59

	B_t1	20 - 112	239	377	384	CL	1.86
	B_k2	112 - 154	198	426	376	SiCL	1.86
12	A_p	0 - 34	575	266	159	SL	1.59
	C_k1	34 - 106	693	224	84	SL	2.03
	C_k2	106 - 156	638	266	96	SL	1.68
13	A_p	0 - 22	321	444	235	L	1.42
	B_k	22 - 72	373	321	306	CL	1.54
	C_k1	72 - 102	423	340	238	L	1.72
	C_k2	102 - 155	387	359	254	L	1.69
14	A_p	0 - 30	366	375	259	L	1.53
	B_{tk}	30 - 114	301	380	319	CL	1.61
	C_k	114 - 152	477	239	284	SCL	1.71

*C: Clay, L: Loam, Si: Silty, S: Sandy**PSD: Particles size distribution, B. Density: Bulk Density

decreases gradually toward the east and southwest this was due to the wide differences in topography and effect of sloping that caused removal of organic matter and increase bulk density and these results accepted with Razvanchy, (2014). The northern part of the study area which is mostly mountainous includes the densest vegetation cover relatively (Al-Quraishi et al., 2020) and affecting on the soil bulk density. Some study soils as in pedon (2 and 10) have high bulk density values at the surface layer because of the sloping effect that caused the removal of organic matter from the surface layer and an increased soil bulk density.

3.1.2. Particles size distribution of the soil

The results of the soil particles size distribution show an increase in clay content in the subsurface and deep horizons comparison with surface horizons in pedons (3, 5, 7, 9, 10, 11, 13, and 14), and this is due to the translocation of clay particles from upper soil horizons. The three main factors that affecting dramatically on the clay translocation from upper to lower horizons are the amount of rainfall, slope degree, and agricultural practices. During field observation and rainfall records we found that the mentioned pedons have various rainfall amounts, therefore, the clay content increasing with depth at different rates depending on the amount of rainfall and intensity in that area, this result agreed with a similar result that was proved by Warrington et al., (2007) when reported differences due to the conditions of each pedon individually. Irrigation has a great effect on clay translocation in irrigated soils. Clay content decreasing with depth in pedons (1, and 2) whereas irregular distribution patterns in pedons (4, 6, 8, and 12). The highest value of clay content was found in (B_{tk}) horizon of pedon (4) with (521 $g.kg^{-1}$) and the lowest value recorded in (C_k1) horizon of pedon 12 with a value of (84 $g.kg^{-1}$). Figure (3) shows the interpolated map for the distribution of clay particles, it appears that higher values of clay particles and fine soil texture are located at the north, northwest, and decreasing into the south and southwest. The highest value of silt is (444 $g.kg^{-1}$) in the pedon (13) (A_p) horizon, and the lowest value is (191 $g.kg^{-1}$) in the pedon (6), (C_k2) horizon. Additionally, the results of silt fraction illustrated no constant distribution pattern and fluctuated between increasing and decreasing in pedons (6, 8, 9, 11, 12, and 13), but the general trend is increased with depth as shown in pedons (1, 2, 5, and 7) whereas in pedons (3, 4, 10, and, 14) silt fraction decrease with depth. These results were proved there is no stable distribution pattern of silt fraction along pedons, this was attributed to the difference in rainfall effect and pedon position. Figure (4) shows the interpolated map for the distribution of silt particles, according to the map the area that has lower silt content is located northeast and increasing toward south and southwest. Silt particles have negative significant correlations with both elevation and slope by (-0.701 and -0.550) respectively. On the other hand, the sand particles increase with depth in pedons (1, 2, 3, 4, 6, 8, 9, 12, 13, and 14) this is due to the existence of sandstone and sandy shale with in situ formation and according to the geological formation of the study area (Sissakian and Fouad, 2012). In contrast, sand fraction decreasing with depth in pedons (5, 7, 10, and 11) this result is supported by a similar result finding of Gul et al., (2011). The highest value of sand particles is (693 $g.kg^{-1}$) for horizon C_k1 in pedon 12, while, the lowest value is (198 $g.kg^{-1}$) for horizon B_k2 pedon (11). Figure (5) shows the interpolated map for the distribution of sand particles, the higher sand content located at the east and increasing irregularly toward the southwest. Sand particles have a positive significant correlation with elevation by (0.576), while no significant correlation with the slope because sand particles were large and not easy translocated by the erosion process.

3.2 Chemical properties

3.2.1 pH and EC

The results of soil chemical properties (Table 3) illustrated that the pH values increased with depth in pedons (1, 2, 4, 5, 6,7, 9, 10, 11, and 13), this result matched with the findings of Filippi et al., (2019), while, in pedons (3, 8, 12, and 14) the pH values decreased with depth, as a result of existing relatively considerable amount of organic matter in subsurface horizons (Table 3) along with the effect of anions in subsurface horizons. The pH values ranged from (7.39-8.60) in (A) horizon of pedon (2) and (C_k2) horizon of pedon (5). Figure (6) shows the interpolated map for studied soil pH distribution as an alkaline from north to south because of derived from the calcareous parent material. The electrical conductivity (EC) values decreasing with depth in pedons (1, 2, 3, 4, 5, 6, 7, 8, and 11), this is due to the continuous leaching process which agrees with Dregne, (1976). While, increasing with depth in pedons (9, 10, 12, 13, and 14).

The low salts content can be attributed to the desalinization process that is affected by rainfall. The highest EC value is (0.783 $dS.m^{-1}$) in pedon (13) C_k2 horizon, as shown in table (3). In contrast, the lowest value is (0.127 $dS.m^{-1}$) in pedon (12) A_p horizon.

The interpolated map of EC show the lowest values located in the middle of the study area and the highest values located at the east, southeast, and southwest locations, this variation of the distribution is due to the parent material of these areas and rainfall effect with topography (Figure 7).

3.2.2 Organic matter

The result of soil organic matter content showed a decrease in depth in all pedons. One of the major reasons for this phenomenon is the accumulation of a relatively high amount of plant residuals (littering process) and adding organic manure at the upper part of the soil, and an increasing the biological activity in biosphere at the root zone, caused decomposition of litter and increasing

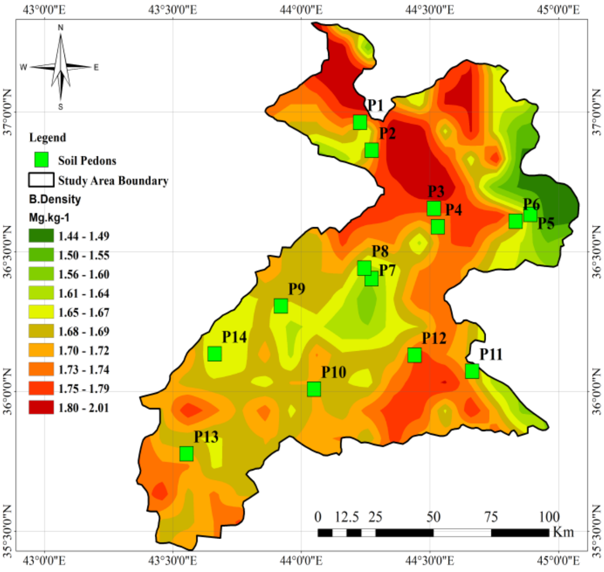

Fig. (2): Interpolated map for soil bulk density (RMS = 0.217)

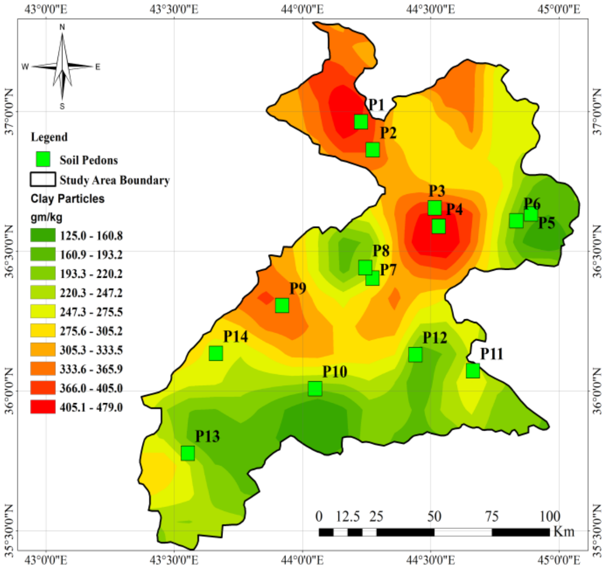

Fig. (3): Interpolated map for clay particles (RMS = 54.11)

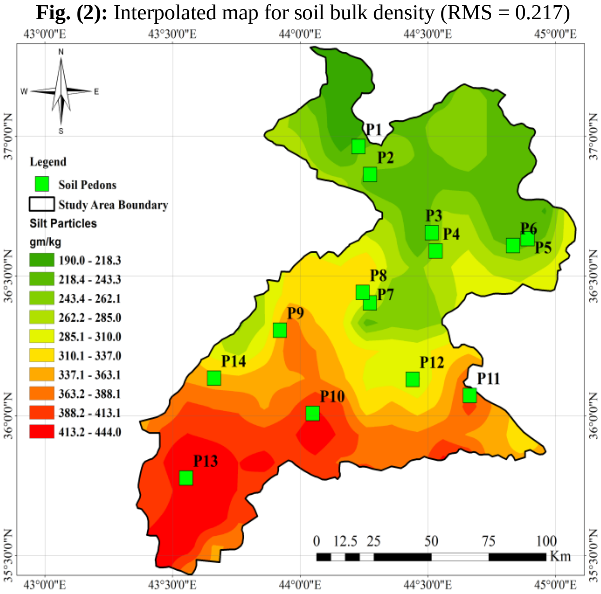

Fig. (4): Interpolated map for silt particles (RMS = 36.31)

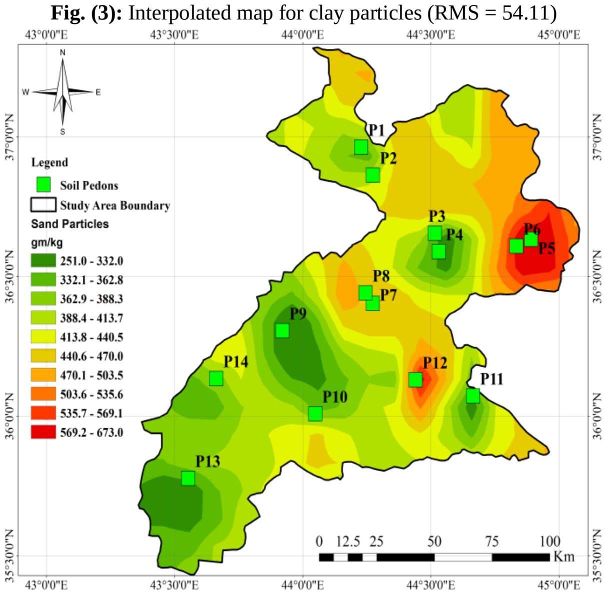

Fig. (5): Interpolated map for sand particles (RMS = 41.47)

humified organic matter at the surface horizon of soil under optimum soil moisture regime and optimum soil temperature regime, since there is a close association between the precipitation, temperature, and the level of soil organic matter as observed by Tate, (1992). Besides it, in pedons (2 and 5) the organic matter content fluctuated with depth, the reasons for these are the addition of organic matter from plant residues (green litter) to topsoil (Adamu and Aliyu, 2012), and addition of the residuals of plant roots to subsurface horizons. However, the decrease of organic matter content was minimal with depth in cultivated land if compared to other land covers. Because of higher organic matter inputs in topsoil, the upper soil layer receives organic matter from the above-ground net primary production and a greater portion of the root production.

Soil organic matter tends to increase as the clay content increases and they have a positive significant correlation by (0.327), this increase is related to two reasons; first, the adhesive between the surface of clay particles and organic matter delay the process of decomposition. Second, soils with a high amount of clay particles increase the potential for aggregate formation, which protects the

hawar.sadiq@su.edu.krd

Table (3): Some chemical properties of studied soils

Pedon no.	Horizon	Depth (cm)	pH	EC dS.m^{-1}	Organic Matter (g.kg^{-1})	Total $CaCO_3$ (g.kg^{-1})	Active $CaCO_3$ (g.kg^{-1})	$CaSO_4.2H_2O$ (%)	Total Nitrogen (g.kg^{-1})	CEC Cmolc.kg^{-1}
1	A_a	0 - 30	8.23	0.345	30.10	332.14	107.40	18.73	3.78	40.43
	C_k1	30 - 80	7.80	0.270	12.04	210.71	105.00	12.91	1.82	34.22
	C_k2	80 - 120	8.39	0.217	8.60	150.00	98.40	9.48	12.60	26.88
2	A	0 - 40	7.39	0.726	17.72	398.21	102.00	20.46	2.80	39.25
	C_k1	40 - 92	7.94	0.236	19.61	375.00	101.40	19.42	4.20	45.81
	C_k2	92 - 140	8.57	0.186	13.93	253.57	96.00	16.86	2.24	38.36
3	A_p	0 - 46	8.00	0.216	28.38	478.57	109.20	14.12	7.28	33.46
	B_k	46 - 126	7.92	0.189	27.52	375.00	100.20	13.60	3.64	32.54
4	A_p	0 - 25	7.61	0.495	20.32	508.93	110.40	15.50	3.64	37.36
	B_{tk}	25 - 57	7.82	0.316	18.92	392.86	108.00	15.83	2.72	42.21
	C_k	57 - 147	8.20	0.198	12.56	339.29	106.92	13.71	2.24	47.12
5	A_a	0 - 25	7.80	0.488	12.73	382.14	105.96	12.52	3.22	18.68
	$C_{hk}1$	25 - 50	7.85	0.205	10.66	425.00	108.00	15.45	2.66	23.59
	C_k2	50 - 120	8.60	0.168	11.70	319.64	106.08	12.47	2.74	42.27
6	A	0 - 28	7.97	0.224	25.61	419.64	106.80	7.64	3.08	28.30
	C_k1	28 - 66	8.01	0.153	11.18	419.64	105.36	12.23	2.80	27.14
	C_k2	66 - 101	8.20	0.156	7.74	357.14	103.44	11.50	4.06	28.81
7	A_a	0 - 65	8.14	0.268	30.96	216.07	93.60	11.91	2.52	40.25
	B_{tk}	60 - 102	8.22	0.241	18.92	303.57	89.28	12.73	1.40	37.89
8	A	0 - 32	8.57	0.329	27.52	348.21	104.40	16.65	5.60	36.90
	B_{tk}	32 - 109	7.81	0.241	20.64	317.86	102.00	17.48	3.08	42.33
	C_k	109 - 179	8.24	0.229	13.76	264.29	97.20	15.15	1.40	43.45
9	A_p	0 - 35	7.69	0.257	12.56	285.71	100.80	12.02	3.36	29.32
	B_{hk}	35 - 100	7.70	0.214	9.98	267.86	104.40	11.55	1.68	26.51
	C_k	100 - 147	8.01	0.284	8.08	250.00	93.60	11.71	1.40	26.14
10	A_p	0 - 23	8.07	0.261	18.92	273.21	95.40	11.41	2.66	29.39
	$B_{tk}1$	23 - 81	8.25	0.236	18.92	217.86	93.60	10.92	5.60	30.21
	$B_{tk}2$	81 - 135	8.17	0.279	6.88	250.00	92.16	10.42	2.80	29.36
11	A_p	0 - 20	7.93	0.451	17.20	232.14	91.32	7.09	2.80	28.84
	B_t1	20 - 112	8.00	0.322	5.16	323.21	94.80	7.09	2.52	25.53
	B_k2	112 - 154	8.15	0.284	5.16	300.00	98.40	9.23	1.54	27.70
12	A_p	0 - 34	8.30	0.127	9.46	335.71	97.20	8.52	1.96	23.05
	C_k1	34 - 106	8.50	0.149	7.74	321.43	99.00	7.11	2.66	27.71
	C_k2	106 - 156	8.17	0.170	5.33	357.14	101.40	8.49	1.40	29.81
13	A_p	0 - 22	7.83	0.545	9.63	278.57	99.60	10.64	2.52	27.93
	B_k	22 - 72	7.91	0.736	8.94	232.14	96.00	10.23	2.52	30.20
	C_k1	72 - 102	7.78	0.783	7.57	250.00	91.20	9.34	2.80	26.80
	C_k2	102 - 155	7.90	0.631	6.36	303.57	98.40	9.16	2.24	28.50
14	A_p	0 - 30	8.13	0.374	17.89	285.71	94.80	12.45	3.58	32.22
	B_{tk}	30 - 114	7.97	0.546	16.17	225.00	108.00	8.80	1.96	37.41
	C_k	114 - 152	8.07	0.498	6.54	241.07	92.40	9.31	2.74	35.56

organic matter from mineralization caused by microbial activity (Rice, 2002). The maximum value of soil organic matter is (30.96 g.kg^{-1}) in A_a horizon, pedon (7), and the minimum value is (5.16 g.kg^{-1}) found in pedon (11) in both horizons B_t1 and B_k2. The interpolated map of organic matter (Figure 8) reveals that the higher values of organic matter content are located north-west and decreases gradually to south and southwest. These changes of organic matter in the study area are related to the vegetation cover, also the amount and distribution of precipitation

hawar.sadiq@su.edu.krd

that they are changing in the same direction (Al-Quraishi et al., 2019). Organic matter has a positive significant correlation with slope by (0.338) because of the dominance of forest trees in different sloping areas (Mountainanous region), whereas no significant correlation with the elevation. Moreover, it has a positive significant correlation with rainfall by (0.538).

3.2.3 Total and active carbonate

The highest value of total carbonate is (508.93 g.kg^{-1}) in pedon (4) horizon (A_p), while, the lowest value is (150.0 g.kg^{-1}) in pedon (1) horizon (C_k2) (Table, 3). The results of total carbonate reveal that there is a decrease in depth in pedons (1, 2, 3, 4, 6, 8, and 9). The

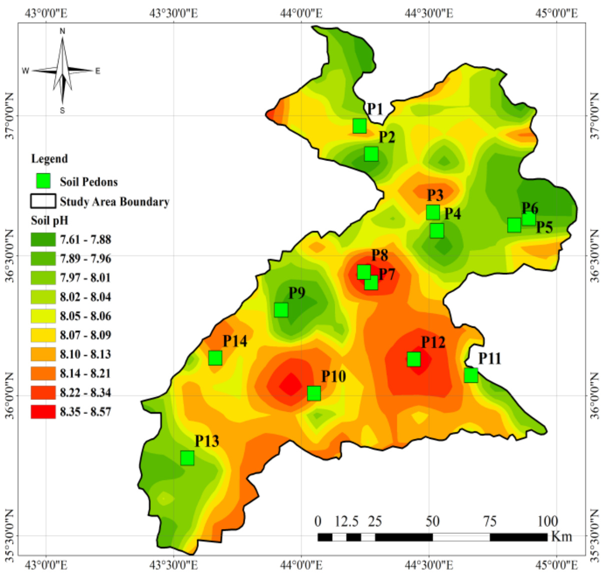

Fig. (6): Interpolated map for soil pH (RMS = 0.322)

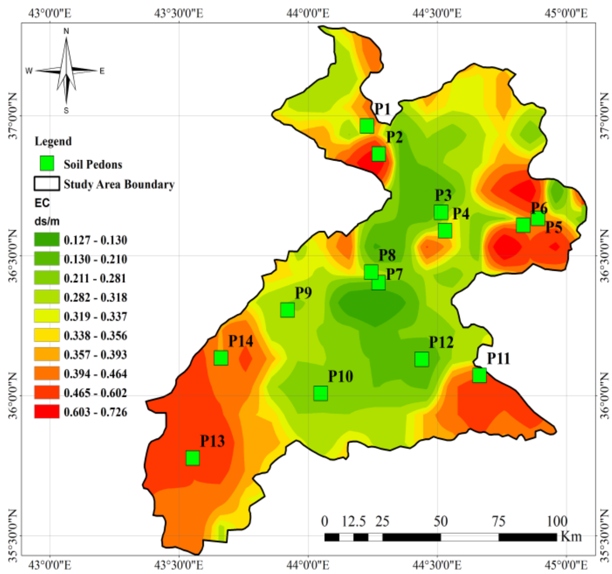

Fig. (7): Interpolated map for EC (RMS = 0.06)

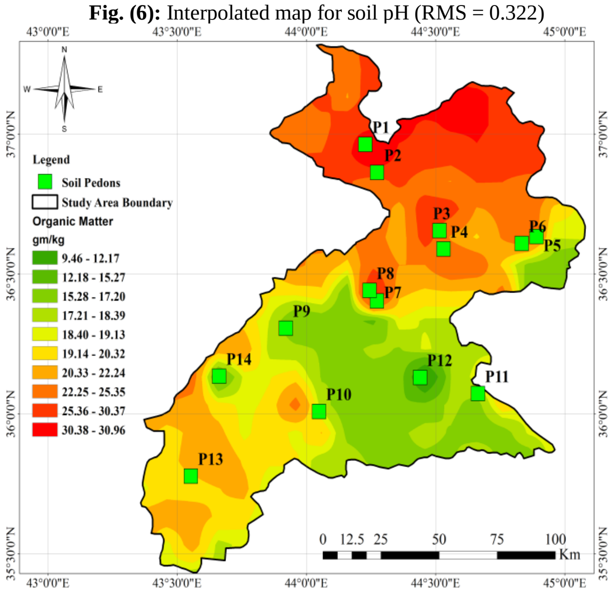

Fig. (8): Interpolated map for OM (RMS = 5.23)

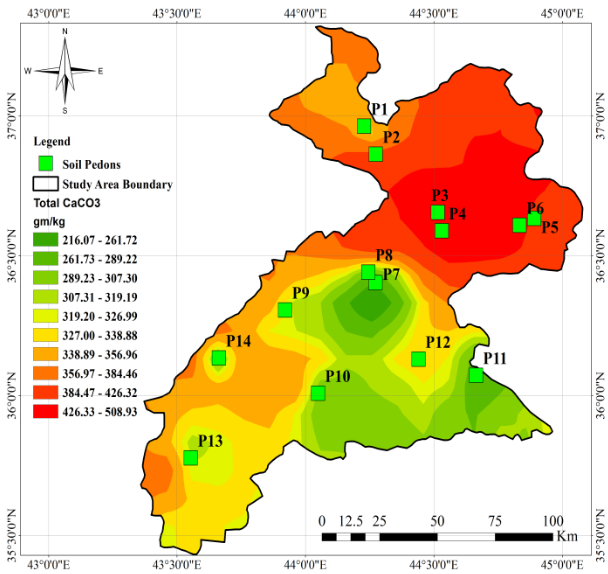

Fig. (9): Interpolated map for total $CaCO_3$ (RMS = 35.10)

decrease of total carbonate with depth is due to the increase of weathering intensity at the surface layer in these study pedons and increase pedogenic carbonate content. In contrast, in pedons (5, 7, 10, 11, 12, 13, and 14) the total carbonate increases with depth this is due to the calcareous parent materials in the (C) horizon which, generally composed of carbonate minerals especially calcite and dolomite as geogenic carbonate, as well as translocation and accumulation of carbonates from upper horizon to lower horizon as a result of gains and losses processes, as well as, wet and dry processes, in addition to in situ formations of carbonate as a result of chemical reactions. The interpolated map of the total carbonate shows (Figure 9) that the highest value is located at north and northeast of the study area and decreasing toward south and southwest, this distribution is due to the topography and rainfall effect. Total carbonate has a positive significant correlation with both slope and elevation by (0.354 and 0.279) respectively.

Active carbonate decrease with depth in pedons (1, 2, 3, 4, 6, 7, 8, 9, 10, and 13), while, increase with depth in pedons (5, 11, 12, and 14). This is due to the translocation of carbonate that is associated with clay and fine silt particles from the upper horizons to lower horizons by rainfall that is affecting to increase the active carbonate with depth. As well as, active carbonate has a strong relationship with clay particles which changes significantly in the same direction as indicated it previously by (0.240). The highest active carbonate value is (110.40 $g.kg^{-1}$) for pedon (4) horizon (A_p), and the lowest value is (91.20 $g.kg^{-1}$) for pedon (13) horizon (C_k1). The distribution of active carbonate (Figure 10) illustrates that the higher amount is located at the northern part of the study area and decreases into two directions south and southwest.

3.2.4 Soil Gypsum

The results of soil gypsum ($CaSO_4.2H_2O$) content reveal that there is a decrease with depth in all pedons except pedons (6, 7, and 11). Gypseous soils contain high concentrations salts that are soluble in water, so it is leach to lower horizons to make the concentration higher with depth. On the other hand, because of its ability to dissolve in water, these salts can easily move under the effect of erosion, this translocation after that to the upper horizons due to capillary force in the hot and dry conditions. The highest gypsum percent is (20.46 %) in pedon (2) horizon (A), and the lowest percentage is (7.09 %) in pedon (11) both horizons (A_p and B_t1). Figure (11) shows the distribution of soil gypsum content through the interpolated map of it, the maximum values located at the northwest direction (around pedon 1 and 2) and decreasing into east, south, and southwest directions. The soil gypsum percent has a positive significant correlation with slope by (0.352), while it has no significant correlation with elevation.

3.2.5 Total nitrogen

Generally, total nitrogen content (TN) decreases with depth for all pedons except in pedons (1, 6, and 10) with some differentiation in subsoil horizons, this distribution pattern is attributed to the existence of nitrogen in organic form, therefore, increase it in surface and subsurface horizons because both of them consider as the zone of accumulation organic matter. On the other hand, in some studied pedons the tillage practice plays a major role in an increase in total nitrogen particularly in a flat area in pedons (9, 11, 12, 13, and 14) that have A_p horizon. Total nitrogen an increase in subsurface horizons as in pedon (1, 6, and 10) due to the effect of decomposition of roots in subsurface horizons and contribute to an increase in total nitrogen. The variation of total nitrogen has been proved through statistical analyses because it changes with organic matter significantly in the same direction by (0.449). The highest value of total nitrogen is (12.60 $g.kg^{-1}$) in pedon (1) horizon (C_k2), and the lowest value is (1.40 $g.kg^{-1}$) found in each of pedon (7) horizon B_{tk}, pedon (8) horizon (C_k), pedon (9) horizon (C_k), and pedon (12) horizon (C_k2). The distribution of total nitrogen in the study area starts with maximum values in the north direction and decreasing almost into all other directions (Figure 12), and an increase in organic matter is one of the major reasons for this increase in total nitrogen at the north direction and then decreases with other directions. Correspondingly, decreases in total nitrogen in other directions related to temperature raising helps the total nitrogen to more volatilizing comparison with north direction, these results agreed with the interpretation of Kulkarni et al., (2015) about total nitrogen.

3.2.6 Cation exchange capacity

The results of CEC reveal that there is an increase with depth in pedons (4, 5, 6, 8, 12, 13, and 14) while decreasing with depth in pedons (1, 2, 3, 7, 9, 10, and 11). Because the CEC depends on clay type and clay content, as well as organic matter content, therefore, the relation of CEC values with depth depends on the changes of these soil properties.

Cation exchange capacity has a positive significant correlation with each of clay particles, and organic matter by (0.262, and 0.479). The CEC values ranged between (18.68 - 47.12 $cmolc.\ kg^{-1}$) in pedon (5) for horizon (A_a) and pedon (4) horizon (C_k), respectively, as shown in the interpolated map of CEC (Figure 13), there is a decrease of CEC from northwest toward the southeast direction as a result of increase organic and mineral colloids at northwest whereas decrease towards the southeast. Additionally, this direction of change is related to the rainfall at the study area that has a positive significant correlation with the CEC by (0.327).

4. CONCLUSIONS

Higher bulk density is located in the north of the study area and decreases gradually toward the east and southwest. Interpolated map for distribution of clay particles appears that higher values of clay particles and fine soil texture are located at the north, northwest, and decreasing into the south and southwest. There is no stable distribution pattern of silt fraction along pedons and have negative significant correlations with both elevation and slope. Soil pH ranged between slightly to moderately alkaline, and the study soils were non-saline. Soil organic matter tends to increase as the clay content increases and they have a positive significant correlation (0.05). The interpolated map of organic matter reveals that the higher values of organic matter content are located at the north-west and decrease gradually to south and southwest. Studied soils have different distribution patterns of total and active carbonates along pedons. Soil gypsum content decrease with depth in most studied pedons. Total nitrogen content decreases with depth for most pedons. CEC decreased from northwest toward a southeast direction.

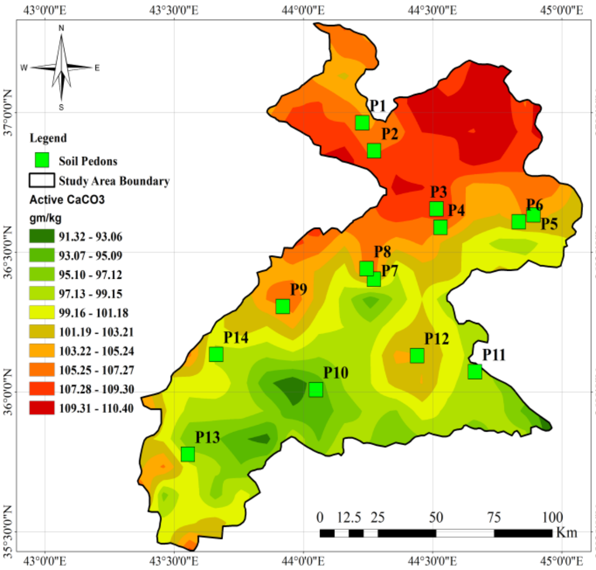

Fig. (10): Interpolated map for active $CaCO_3$ (RMS = 9.83)

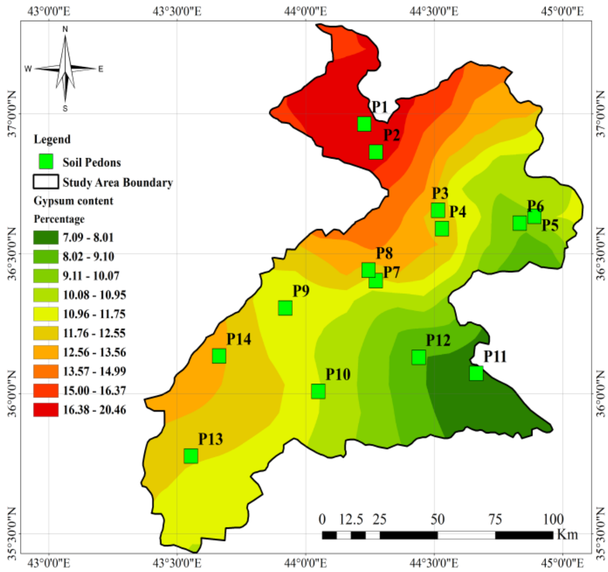

Fig. (11): Interpolated map for $CaSO_4$ (RMS = 2.35)

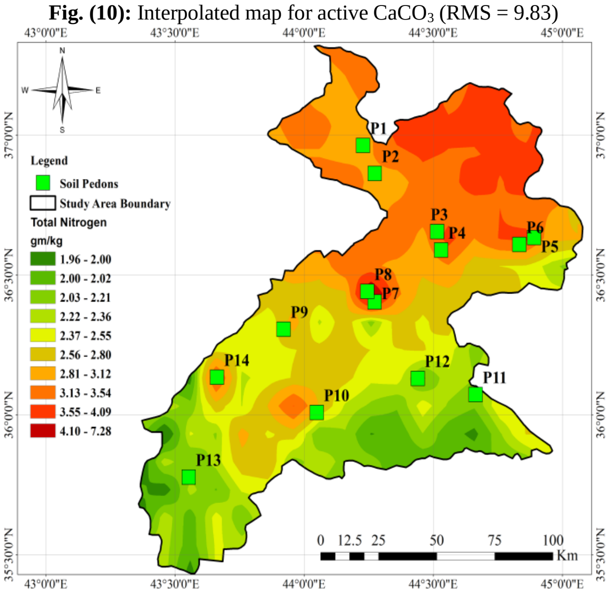

Fig. (12): Interpolated map for soil TN (RMS = 0.83)

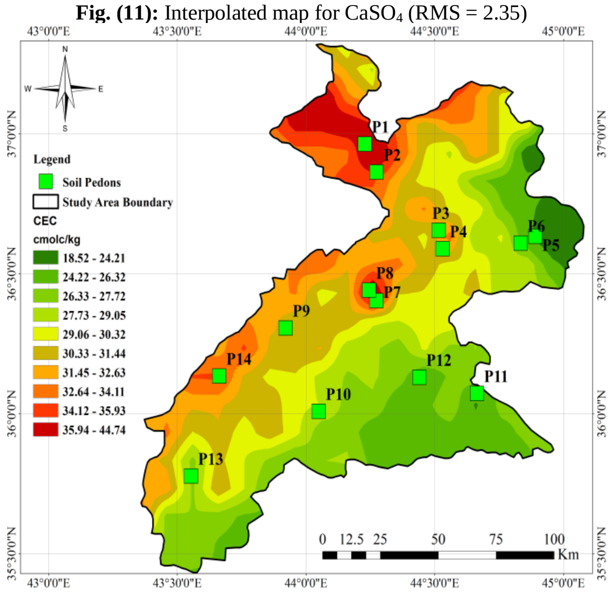

Fig. (13): Interpolated map CEC (RMS = 4.20)

5. REFERENCES

Adamu, G. and Aliyu, A. 2012. Determination of the influence of texture and organic matter on soil water holding capacity in and around Tomas Irrigation Scheme, Dambatta Local Government Kano State. Research Journal of Environmental and Earth Sciences, 4, 1038-1044.

Al-Quraishi, A., Razvanchy, H. and Gaznayee, H. 2020. A Comparative Study for Performance of Five Landsat-based Vegetation Indices: Their Relations to Some Ecological and Terrain Variables. Journal of Geoinformatics & Environmental Research, 1, 20-37.

Al-Quraishi, A. M. F., Sadiq, H. A. and Messina, J. P. 2019. Characterization and modelling surface soil physicochemical properties using Landsat images: a case study in the Iraqi Kurdistan region. International Archives of the Photogrammetry, Remote Sensing and Spatial Information Sciences. XLII-2/W16, 21-28

Babbie, E. R. 2009. The Practice of Social Research. 12th ed. 94-106.

Baharom, S. N. A., Shibusawa, S., Kodaira, M. and Kanda, R. 2015. Multiple-depth mapping of soil properties using a visible and near infrared real time soil sensor for a paddy field. Engineering in Agriculture, Environment and Food, 8, 13-17.

Black, C. A. 1980. Methods of Soil Analysis Madison, Wisconsin. USA, Soc.Agron. Inc Publishers. 155-157,167-171.

Bockheim, J., Munroe, J., Douglass, D. and Koerner, D. 2000. Soil development along an elevational gradient in the southeastern Uinta Mountains, Utah, USA. Catena, 39, 169-185.

Bremner, J. M. and Mulvaney. C. S. 1982. Nitrogen -Total: 595-622. In A.L. Page et al., (ed.) Methods of soil analysis. Part 2. Chemical and microbiological properties. Agron. Monogr. 9. ASA, Madison, WI.

Brubaker, S., Jones, A., Lewis, D. and Frank, K. 1993. Soil properties associated with landscape position. Soil Science Society of America Journal, 57, 235-239.

Carter, M. R. And Gregorich, E. G. 2007. Soil sampling and methods of analysis, CRC press. 44-48.

Congalton, R. G. and Green, K. 2019. Assessing the accuracy of remotely sensed data: principles and practices, CRC press. 103-118.

Donovan, P. 2012. Measuring soil carbon changes A flexible, practical, local method. 91-103.

Filippi, P., Jones, E. J., Ginns, B. J., Whelan, B. M., Roth, G. W. and Bishop, T. F. 2019. Mapping the depth-to-soil pH constraint, and the relationship with cotton and grain yield at the within-field scale. Agronomy, 9, 251.

Gee, G. and Bauder, J. 1986. Particle-size analysis.

Gul, H., Khattak, R., Muhammad, D. and Shah, Z. 2011. Physical properties of soils under sub-surface drainage system. J Agric, 27, 225-232.

Tropical Forests. 64-73.

Hyndman, R. J. and Koehler, A. B. 2006. "Another look at measures of forecast accuracy". International Journal of Forecasting. 22 (4): 679–688.

Iqbal, J., Read, J. J., Thomasson, A. J. and Jenkins, J. N. 2005. Relationships between soil-landscape and dryland cotton lint yield. Soil science society of America journal. 69, 872.

Ismail, H. K. 2013. Significance of climosequence on genesis, development and mineralogy of some selected soils from Iraqi Kurdistan Region. MSc thesis, soil and water science dept., College of Agriculture, University Of Duhok.

Kozhekov, O. K. and N. A. Yakovleva. 1977. Determination of carbonates and carbonate minerals in soils. Soviet Soil Sci. 9:620-622.

Kravchenko, A. N. and Bullock, D. G. 2000. Correlation of corn and soybean grain yield with topography and soil properties. Agronomy Journal, 92, 75-83.

Kulkarni, M. V., Groffman, P. M., Yavitt, J. B. and Goodale, C. L. 2015. Complex controls of denitrification at ecosystem, landscape and regional scales in northern hardwood forests. Ecological Modelling, 298, 39-52.

Kumhálová, J., Kumhála, F., Kroulík, M. and Matějková, Š. 2011. The impact of topography on soil properties and yield and the effects of weather conditions. Precision Agriculture, 12, 813-830.

Rice, C. W. 2002. Organic matter and nutrient dynamics. Encyclopedia of soil science, 2, 1180-1183.

Razvanchy, H.A.S. 2014. Modelling some of the Soil Properties in the Iraqi Kurdistan Region using Landsat Datasets and Spectroradiometer. MSc thesis, soil and water science dept., College of Agriculture, Salahaddin University-Erbil.

Rowell, D. L. 1994. Soil science: methods and applications, Harlow, Longman Group Limited, Longman Scientific and Technical. 53-70.

Sissakian, V. K. and Fouad, S. 2012. Geological map of Iraq, scale 1: 1000000. Iraq Geological Survey (GEOSURV) publications, Baghdad, Iraq. 4-6.

Tate, K. 1992. Assessment, based on a climosequence of soils in tussock grasslands, of soil carbon storage and release in response to global warming. Journal of Soil Science, 43, 697-707.

Warrington, D. N., Goldstein, D. and Levy, G. 2007. Clay translocation within the soil profile as affected by intensive irrigation with treated wastewater. Soil science, 172, 692-700.